Substrate-specific presentation of MHC class I-restricted antigens via autophagy pathway

Maria Tovar Fernandez, Ewa Sroka, Mathilde Lavigne, Aikaterini Thermou, Chrysoula Daskalogianni, Bénédicte Manoury, Rodrigo Prado Martins, Robin Fahraeus

Version of Record: https://www.sciencedirect.com/science/article/pii/S0008874922000089
Manuscript_201b6b3ab8c3ddce503c66bbdd85a427

Substrate-specific presentation of MHC class I-restricted antigens via autophagy pathway.

Maria C. Tovar Fernandez[1,2], Ewa M. Sroka[1,2,*], Mathilde Lavigne[1,*], Aikaterini Thermou[1,2] Chrysoula Daskalogianni[1,2], Bénédicte Manoury[3], Rodrigo Prado Martins[1,4] and Robin Fahraeus[1,2,5,6,8]

[1]Inserm UMRS1131, Institut de Génétique Moléculaire, Université Paris 7, Hôpital St. Louis, F-75010 Paris, France

[2]ICCVS, University of Gdańsk, Science, ul. Wita Stwosza 63, 80-308 Gdańsk, Poland

[3]Institut Necker Enfants Malades, INSERM U1151-CNRS UMR 8253, Université de Paris, Faculté de Médecine Necker

[4]ISP, INRAE, Université de Tours, UMR1282, Tours, Nouzilly, France

[5]Department of Medical Biosciences, Building 6M, Umeå University, 901 85 Umeå, Sweden

[6] RECAMO, Masaryk Memorial Cancer Institute, Zluty kopec 7, 65653 Brno, Czech Republic.

[8] To whom correspondence should be addressed: robin.fahraeus@inserm.fr

• These authors contributed equally.

Key words: MHC class I restricted antigen presentation; autophagy; protein aggregates; EBV-encoded EBNA1

Declarations of interest: none

Highlights

• Substrate restricted presentation of MHC class I antigens via Atg5/12-dependent autophagy.
• Suppression of autophagy-mediated antigen presentation by the gly-ala repeat of the EBV-encoded EBNA1
• Poly glutamine (polyQ)-induced protein aggregates are not presented to the MHC class I pathway via autophagy.

Abstract

The accumulation of protein aggregates is toxic and linked to different diseases such as neurodegenerative disorders, but the role of the immune system to target and destroy aggregate-carrying cells is still relatively unknown. Here we show a substrate-specific presentation of antigenic peptides to the direct MHC class I pathway via autophagy. We observed no difference in presentation of peptides derived from the viral EBNA1 protein following suppression of autophagy by knocking down Atg5 and Atg12. However, the same knock down treatment suppressed the presentation from ovalbumin. Fusing the aggregate-prone poly-glutamine (PolyQ) to the ovalbumin had no effect on antigen presentation via autophagy. Interestingly, fusing the EBNA1-derived gly-ala repeat (GAr) sequence to ovalbumin rendered the presentation Atg5/12 independent. We also demonstrate that the relative levels of protein expression did not affect autophagy-mediated antigen presentation. These data suggest a substrate-dependent presentation of antigenic peptides for the MHC class I pathway via autophagy and indicate that the GAr of the EBNA1 illustrates a novel virus-mediated mechanism for immune evasion of autophagy-dependent antigen presentation.

Introduction

The cellular $CD8^+$ T cell immune response is based on the recognition of antigenic peptides presented on the surface of host cells on the major histocompatibility complex (MHC) class I molecules. The presentation of antigenic peptides via the direct MHC class I pathway involves the degradation of the substrate by the proteasome, transport into the endoplasmic reticulum and further processing by peptidases and loading onto the MHC I molecules [1,2]. On the other hand, exogenous antigens endocytosed by professional presenting cells, such as dendritic cells or macrophages, are translocated to endosomal compartments and presented to the MHC I pathway via the so-called cross presentation pathway [1]. It was thought early on that peptides for the MHC I & II pathways were derived from processing of full length proteins but studies have since discovered a more complex origin of MHC-I antigenic peptides, including peptides derived from the 3' untranslated sequences (UTRs) of mRNAs [3] and from introns [4–6], supporting a model in which non-canonical translation can provide antigenic peptide substrates.

The latent Epstein-Barr (EBV) and Kaposi's sarcoma viruses both target mRNA translation to evade the MHC-I pathway [7,8]. The EBV-encoded EBNA1 uses a glycine-alanine repeat (GAr) consisting of small non-polar amino acids that is prone to cause aggregates [9,10]. The GAr suppresses translation of any mRNA to which it is fused and this has been shown to minimize the presentation of antigenic peptides for the direct MHC class I pathway [7] . It consists of a stretch of up to 250 single glycine residues separated by one, two or three alanines. Inserting a single serine in every eight residue renders the GAr non-functional [11]. EBNA1 has been reported to be presented to the class II pathway via autophagy [12] but whether, or not, peptides for the class I pathway can be generated from processing of full length proteins via

autophagy remains an open question. A cross-presentation study reported MHC I molecules on endolysosomal compartments [13] and it was suggested that endogenous human cytomegalovirus latency-associated protein (pUL138) can be presented to $CD8^+$ T cells through autophagy [14].

The poly glutamine (PolyQ) is well known to cause aggregates to which it is fused and is implicated in various neurodegenerative diseases such as Huntington disease (HD), dentatorubral pallidoluysian atrophy (DRPLA), spinobulbar muscular atrophy (SBMA) and six spinocerebellar ataxias (SCA) [15].

Autophagy is a key degradative process of endogenous cytoplasmic proteins [16,17]. It was first defined as non-specific degradation process, but it was later revealed that autophagy has selectivity for specific cargos including, but not exclusively, aggregated proteins tagged with ubiquitin chains that are recognized by autophagy receptors bound to the autophagosomes membrane protein LC3 (Light chain 3)[18–20]. There are different autophagy such as microautophagy, chaperon mediated autophagy and macroautophagy [21]. In this study, we focused on the macroautophagy pathway that has been implicated in presenting EBNA1 to the class II pathway [12]. It involves the recruitment of ATG proteins, such as Atg5 and 12, to specific phagophore assembly sites (PAS) that elongates and traps a portion of the cytosol until it is sealed in the double membrane autophagosome vesicle. After trapping the engulfed cytosolic cargo, autophagosomes fuse to the lysosome to clear the cargo and the autophagic body [20]. It was recently proposed that the trafficking route of autophagosomes carrying cytoplasmic molecules fuse with endosomes carrying MHC class II molecules and thereby facilitate presentation of endogenous antigens on MHC II molecules [22].

In this study we have used the EBNA1 protein that is known to be processed by the autophagy pathway as well as protein aggregates caused by the poly-glutamine (PolyQ) repeat to address if autophagy is a source of peptide substrates for the MHC class I pathway.

Material and Methods

Plasmids

The pCDNA3-EBNA1, pCDNA3-EBNA1ΔGAr, pCDNA3-Ovalbumin (OVA), pCDNA3-GAr-OVA and pCDNA3-*c-myc* GAr-OVA constructs were obtained as described previously [23].

c-myc EBNA1 and *c-myc* EBNA1ΔGAr were generated by amplification of full-length human *c-myc* by polymerase chain reaction (PCR), using a 5' sense primer containing a HindIII site 5' AAT**AAGCTT**CCACTGCTTACTGGCTTATCG 3' and a 3' antisense primer 5' TAA**AAGCTT**CGGCCGTTACTAGTGGATCC 3' containing another HindIII site. The fragment was cloned into the 5'UTR digested pCDNA3-EBNA1 and EBNA1ΔGAr constructs.

The OVA Poly 125 glutamine (Q) construct was made by digestion of OVA construct with EcoRI and XbaI enzyme and introducing 125 glutamine repetition sequence contained in a vector already mentioned previously [24].

Cell culture and Transfection

H1299 cells (Human non-small cell lung carcinoma) were cultured in RPMI-1640, supplemented with 10% fetal bovine serum (FBS), 2mM L-glutamine and 1% Penicillin- Streptomycin and mouse cell atlas (MCA-205) cells were cultured in RPMI-1640, supplemented with 10% fetal bovine serum (FBS), 2mM L-glutamine, 1% non-

essential amino acids, 1% sodium pyruvate and 1% Penicillin-Streptomycin. For antigen presentation experiments, cells were cultured in 6 wells plates ($8x10^4$ cells/well) at 37˚C with 5% CO_2. The day after seeding and Atg5/12 siRNA induction, transfections were performed using 3 µl of Gene Juice reagent according to the manufacture's protocol (Merck Bioscence). Cells were co-transfected with 0.5 µg of murine MHC class I molecule Kb and 1 µg of EBNA1, EBNA1ΔGAr, GAr-OVA and PolyQ-OVA cDNA carrying the SIINFEKL (SL8) epitope coding sequences in its open reading frame (ORF). In all antigen presentation assays, 1 µg of an OVA cDNA was used as positive control and the same quantity for the empty vector as negative control.

siRNA against Atg5/12

The day after seeding, cells were transfected with Human siRNAs or Murine siRNAs at 20 pM using Jet Prime reagent (Polyplus) following the manufacturer's instructions. The knock down of these proteins was evaluated by Real time PCR (qRT-PCR) and Western Blot at the end of 72 hours incubation and 120 hours.

Human siRNAs used were: two siRNAs against Atg12 (SI02655289 and SI04335513, Qiagen) and three siRNAs against Atg5 (SI02655310, SI02633946 and SI00069251, Qiagen).

Murine siRNAs used were: two siRNAs against Atg12 (SI00900319|S0 and SI00900333|S0, Qiagen) and three siRNAs against Atg5 (SI02696806|S0, SI02720186|S0 and SI02745435|S0, Qiagen).

Chloroquine treatment

The day after seeding, cells were treated with Chloroquine at [30µM] during 36 hours. The autophagy inhibition was evaluated by Western Blot assessing LC3-II accumulation.

Antigen Presentation assay: OT1 CD8$^+$ T cells proliferation

To determine the levels of antigen presentation, we used CD8$^+$ T cells that express specific receptors to the OVA epitope, SIINFEKL, recognized by H-2 Kb. These CD8$^+$ T cells were purified from OT1 transgenic mice expressing a transgenic TCR specific for SIINFEKL-Kb. Spleen and lymph nodes from OT1 transgenic mice were passed through a 70 µm cell strainer and red blood cells were lysed with ACK buffer treatment during 5 minutes. After several washes with PBS-FBS 5%, CD8$^+$ T cells were negatively selected using a CD8$^+$ T cell isolation kit (MACS Miltenyi Biotec) according to manufacturer's instructions. Afterwards, the CD8$^+$ T cells were stained with CellTrace™ Violet at 5µM during 10 minutes (Thermo Fisher Scientific, USA) according to the manufacturer's protocol.

Two days after transfection, H1299 cells used as presenting cells were briefly washed with PBS, trypsinized, resuspended in splenocytes medium (RPMI-1640), supplemented with 10% (FBS), 4mM L-glutamine, 1% Penicillin-Streptomycin, 0.05 mM 2-Mercaptoethanol and 5 mM HEPES) and seeded in 48 wells plates ($1.25x10^5$) cells per well. Then, $5x10^5$ CellTrace™ labelled T-cells were added per well and the co-cultures were incubated at 37°C with 5% CO_2. The levels of antigen presentation were deduced from the percentage of T-cell proliferation verified by flow cytometry.

Flow Cytometry analysis: OT1 CD8$^+$ T cells proliferation

After 3 days, cells were harvested, stained with anti-mouse CD45.2-PE-Cy7 (BD Pharmingen), fixable viability dye eFluor® 506 (eBioscience, USA) and analyzed on a CANTO II flow cytometer (BD Biosciences, USA). Cells were gated for live CD45.2+ cells ($4x10^5$ events collected) and data was analyzed using FlowJo software version 8 (Tree Star). The percentage of live $CD8^+$ T cells in each generation was calculated using FlowJo proliferation platform and this value was considered for statistical analysis.

Antigen Presentation assay: Direct measurement in the presenting cells

H1299 cells co-expressing murine MHC I Kb and the constructs mentioned above were submitted to Chloroquine treatment. Then, cells were harvested and stained with APC anti-mouse H-2 Kb bound to SIINFEKL Antibody (Biolegend) and Fixable viability 506 (eBioscience, USA). These cells were analyzed on a CANTO II flow cytometer (BD Biosciences, USA) and were gated for live cells. Data was analyzed using FlowJo software version 8 (Tree Star).

Direct measurement of MHC I Kb and HLA-ABC

MCA-205 and H1299 cells were submitted to murine or human Atg5/12 siRNA transfection. Then, cells were harvested and stained. MCA-205 cells with anti-mouse H-2 Kb Antibody (Biolegend) and FITC anti-mouse IgG2a Antibody (Biolegend); H1299 cells with HLA-ABC FITC antibody (Invitrogen). Both cell types were also stained with Fixable viability 780 (eBioscience, USA). These cells were analyzed on a CANTO II flow cytometer (BD Biosciences, USA) and were gated for live cells. Data was analyzed using FlowJo software version 8 (Tree Star).

RNA extraction, RT-PCR and qRT-PCR

At 72 hours post siRNA Atg5/12 transfection, H1299 cells were washed with PBS and RNA was purified using the RNeasy Plus Mini Kit (Qiagen) following the manufacturer's protocol. cDNA synthesis was carried out using M-MLV reverse transcriptase and oligo(dT) primers (Invitrogen). For qRT-PCR, the StepOne (Applied BioSystems) real-time PCR system was used, and the reactions were performed with the Perfecta SYBR green Fast mix ROX (Quanta) using specific primer pairs for human Atg5 (Forward: 5' GCTGCAGATGGACAGTTGCA 3'and Reverse: 3' TGTTCACTCAGCCACTGCAG 5'), human Atg12 (Forward: 5' ATGACTAGCCGGGAACACCA 3' and Reverse : 3' CACGCCTGAGACTTGCAGTA 5'), murine Atg5 (Forward: 5'TGTGCTTCGAGATGTGTGGTT 3'and Reverse: 3' GGTCCCCTTTGCACACTTACA 5') and murine Atg12 (Forward: 5'GCCATCTCACCAGCCCAATA 3' and Reverse: 3'CATGCCTGGGATTTGCAGT 5').

LC3-GFP induction

To confirm the blockage of autophagosomes formation by Atg5 and Atg12 siRNA, we performed epifluorescence microscopy. For this, we seeded 1.5 x 10^4 H1299 cells in a 24 well plate over a sterile 22x22mm cover slip. Then, cells were transfected with 20 pM of siRNA against Atg5/12 and 0.1 µg of a LC3-GFP construct at 24 and 48 hours after seeding, respectively. After 72 hours of culture, cells were treated with a starvation buffer described elsewhere [25](140 mM NaCl, 1 mM CaCl2, 1 mM MgCl2, 5 mM glucose, and 20 mM Hepes, pH 7.4) during 2 hours and complete RPMI-1640 medium was used for the negative control cells. Images were taken at 63x using the Axio Imager D2 microscope. All images were analyzed in Fiji software and the number of green dots was calculated as previously described [26].

Western Blot

Cells were trypsinised and the obtained pellets were resuspended with 50 µl of lysis buffer (20 mM HEPES KOH, 50mM β-Glycerol phosphate, 1mM EDTA, 1mM EGTA, 0.5mM Na3VO4, 100 mM KCL, 10% Glycerol and 1% Triton x-100, protease inhibitor cocktail Roche). Total lysates were obtained after mechanic hitting and freezing at -80°C for at least 2 h. After, samples were centrifuged at 13 000 RCF during 10 min at 4°C and supernatants were collected. Samples were quantified using Bradford Reagent (BioRad) and 50 µg of protein were separated on 4-12% SDS-PAGE gels (Thermo Fisher Scientific) and transferred to nitrocellulose blotting membranes (Pall Corporation). After saturation of membranes with TBS- 0.5% Tween containing 5% non-fat milk, membranes were overnight incubated with anti-EBNA1 (16216-1-AP Abnova), anti-Atg12 (R&D systems), anti-chicken egg albumin (C6534 Sigma), anti-LC3B (L75443 Sigma), anti-GFP (11814460001 Roche) and anti-actin (AC-15 Sigma) antibodies. After washing with TBS-Tween, bound antibodies were detected using a rabbit anti-mouse (Dako) or a mouse anti-rabbit (Dako) secondary antibody conjugated to horseradish peroxidase (1:1000; 1 h at room temperature). Immunocomplexes were then revealed with ECL (Thermo scientific) and imaged using a MyECL Imager (Thermo scientific).

Immunofluorescence

H1299 cells were seeded as described for LC3-GFP induction experiments and transfected with 0.8 µg of EBNA1, EBNA1ΔGAr, GAr-OVA, EBNA1 *c-myc*, EBNA1ΔGAr *c-myc*, GAr-OVA *c-myc*, OVA, PolyQ-OVA or empty vector. Samples were fixed with 4% paraformaldehyde and permeabilized with 0.4% Triton x-100 0.05% CHAPS PBS. Afterwards, cells were blocked with 3% Bovine serum albumin (BSA) Saponin 0.1% PBS during 1 hour and then incubated with mouse anti-EBNA1 (16216-1-AP Abnova) or rabbit anti-egg albumin (C6534 Sigma) during 1 hour at

room temperature. After two washes with PBS, samples were incubated with an anti-mouse Alexa 488 or anti-rabbbit Alexa 647 antibodies during 1 hour at room temperature. Next, samples were washed with PBS, stained with DAPI and mounted with a fluorescence mounting media (Dako). Samples were examined in a LSM 800 confocal laser microscope (Carl Zeiss MicroImaging GmbH, Jena, Germany) and images were treated using the Fiji software.

Statistics

Data were analyzed by two-tailed unpaired Student's t-test or One sample T-test using GraphPad Prism 6 for Windows (GraphPad Software). Data shown are mean ± sd. of minimum three independent experiments. *P < 0.0332; **P < 0.0021; ***P < 0.0002; ****P < 0.0001; 0,1234 ns, not significant.

Results

Knocking down Atg5 & Atg12 blocks autophagy in H1299 cells.

In order to evaluate the role of autophagy in antigen presentation to the MHC class I pathway we knocked down the expression of Atg5 and Atg12 using specific siRNAs. These proteins are crucial in the conjugation system that allows the formation of autophagosomes and their downregulation is reported to block the macroautophagy pathway (from here on simply referred to as autophagy) [12,27,28]. The efficiency of siRNA treatments was confirmed by the downregulation of Atg5/12 at both mRNA (**Fig. 1A**) and protein levels (**Fig. 1B, upper lane**). siRNA treatments resulted in a decrease of LC3 II-I ratio (**Fig. 1B, middle lane**) and suppressed autophagy flux following serum deprivation (**Fig. 1C, upper part**) Of note, LC3-GFP protein levels did not change under serum starvation (**Fig. 1C, bottom part**). Together, these data

show that the siRNA against Atg5/12 interfere with the autophagy pathway in H1299 cells.

Preventing autophagy reduces MHC class I antigen presentation independently of protein aggregate formation.

Autophagy can degrade harmful cytosolic protein, including aggregates, [18–20] and we tested the capacity of this pathway to process protein substrates for the MHC-I pathway. We used a chicken OVA construct whose secretion was blocked by the deletion of the first 50 amino acids [29]. This construct enabled us to study the antigen presentation via the MHC-I pathway using $CD8^+$ T cells from OT-1 mice that specifically recognize the OVA-derived SL8 antigenic peptide in the context of the murine Kb MHC class I molecule. We also used a poly-glutamine repetition (PolyQ), well known to cause aggregates and to be processed by autophagy [30–33] that we fused to OVA (**Fig. 2A**). We used a GFP construct to estimate transfection efficiency of approximately 30% to 50% of cells (**Suppl. Fig 1**). Immunohistochemistry assays using anti-OVA antibodies showed that PolyQ-OVA forms approximately 10 aggregates per cell (white arrow heads) while OVA was uniformly stained throughout the cells and no visible aggregate detected (**Fig. 2B**). Expression of the reporter constructs were not significantly affected by siRNA against ATG5/12 (**Fig. 2C and suppl. Fig. 2**). We did not detect an accumulation of PolyQ-OVA upon ATG5/12 knock down, presumably due to the fact that the PolyQ-OVA is not present only in the aggregate conformation (**Fig. 2B**) due to the limited time (24 hours) of expression. To test the role of autophagy on the processing of antigenic peptide substrates for the MHC class I pathway, we co-expressed the indicated SL8-carrying constructs together with the Kb MHC cDNA in human H1299 cells. Transfected cells were subject to autophagy inhibition through Atg5/12 siRNA treatment and antigen

presentation was evaluated by co-culture with OT1 CD8$^+$ T-cells. The relative level of antigen presentation was estimated by OT1 CD8$^+$ T-cells proliferation using flow cytometry. For every assay we confirmed suppression of autophagy by in parallel estimating the LC3 I/II ratio (Fig. 1B and data not shown). We observed that under Atg5/12 knock down, OVA and PolyQ-OVA showed a higher percentage of cells in the non-proliferating OT1 CD8$^+$ T cell population (G0) and a corresponding decrease in the proliferating population (G1 to G5), indicating a reduction of antigen presentation (**Fig. 2D**). The percentage of OT1 CD8$^+$ T cells in each generation is shown in (**Suppl. Fig. 3A)**. Despite being uniformly expressed and showing no apparent formation of aggregates, it was surprising to see that knocking down Atg5/12 affected the presentation of antigenic peptides from OVA as much as from PolyQ-OVA.

MHC class I-restricted presentation of peptides derived from EBNA1 is not affected by suppressing autophagy.

The Epstein-Barr virus-encoded EBNA1 has been reported as an aggregate prone protein and this feature has been attributed to the long repeat of non-polar gly-ala residues (GAr) [9,10]. Since EBNA1-derived antigenic peptides are processed for the MHC class II pathway via autophagy [12] and autophagy is associated to the clearance of proteins, including aggregates [18–20], we wanted to know if EBNA1-derived peptides can also be presented for the MHC class I pathway through autophagy. We inserted the antigenic SL8 peptide into the EBNA1 open reading frame (ORF), or in an EBNA1 depleted of the GAr-domain (EBNA1ΔGAr). We also used a construct carrying the GAr-domain fused to OVA cDNA (GAr-OVA) (**Fig. 3A**). To test if EBNA1 shows the same aggregation pattern observed for PolyQ-OVA, we performed immunohistochemistry assays. However, we observed no obvious

aggregates of EBNA1, EBNA1ΔGAr or GAr-OVA and no differences in subcellular localisation with, or without, the GAr (**Fig.3B**). The GAr mediates suppression of antigenic peptides for the MHC class I pathway by inhibiting *EBNA1* mRNA translation *in cis* [7]. In agreement with this, we observed a low percentage of $CD8^+$ T cell proliferation in response to SL8 derived from EBNA1 and GAr-OVA, as compared to EBNAΔGAr (**Fig. 3C**) and OVA (**Fig.2D**). Importantly, we observed no significant difference between percentages of OT-1 $CD8^+$ T cells in the undivided (G0) or in the proliferating populations (G1 to G5), for any of the tested conditions following Atg5/12 siRNA treatment (**Fig. 3C** and **suppl. Fig. 3B**). We also showed that Atg5/12 knock down had no significant effect on EBNA1, EBNA1ΔGAr and GAr-OVA expression (**Fig. 3D** and **suppl. Fig. 2**). In addition, we observed no effect on antigen presentation of EBNA1, EBNA1ΔGAr or GAr-OVA following treatment with the autophagy inhibitor drug Chloroquine (**Suppl. Fig. 4**). These results support the idea that the autophagy pathway does not provide EBNA1-derived antigenic peptides for the class I pathway and that the fusion of the GAr prevents OVA from being presented via autophagy.

The level of protein expression does not determine MHC class I restricted antigen presentation via the autophagy pathway.

The above results were surprising considering that OVA alone, or OVA fused to the PolyQ, present antigenic peptides in an Atg5/12-dependent fashion, while this antigen presentation pathway is prevented by the fusion of the GAr. We next set out to test if the effect of the GAr on antigen presentation is associated with its effect on suppressing mRNA translation *in cis*. For this we fused the *c-myc* 5'UTR to the 5' of the EBNA1, EBNAΔGAr and GAr-OVA (**Fig. 4A**). The presence of the *c-myc* sequence overcomes the translation inhibitory capacity of the GAr and restores

protein synthesis without altering the coding sequence [23]. Western blots and Immunofluorescence showed that the insertion of the *c-myc* sequence resulted in the expected increase in expression of EBNA1 and GAr-OVA but not EBNAΔGAr (**Fig. 4B** and **suppl. Fig.5A)**, and did not affect the subcellular localization (**Fig. 4C**). Atg5/12 knock down did not affect the expression of either construct (**Fig. 4D and suppl. Fig. 2).** When we compared antigen presentation we observed the expected increase in presentation from the *c-myc*-carrying GAr-OVA construct, as compared to GAr-OVA alone (**Suppl. Fig.5B**). Importantly, there was no significant difference in antigen presentation between *c-myc* carrying constructs following Atg5/12 knock down. (**Fig. 4E and suppl. Fig. 3C**). These results show that the levels of protein expression do not affect autophagy-dependent presentation of antigenic peptides derived from EBNA1 or from GAr-Ova for the MHC class I pathway.

Discussion

Alternative sources of peptides for the MHC class I pathway have been proposed but if, and to what extent, peptides derived from the processing of peptide substrates via the autophagy pathway can be presented to the class I pathway is poorly investigated. The PolyQ sequence is linked to several neurodegenerative diseases, including Huntington's disease, and is well known to cause aggregates of proteins to which it is fused [15,34]. The GAr is a disordered domain derived from the EBNA1, a viral protein expressed in all Epstein-Barr virus (EBV)-infected cells [35], and known to cause aggregates [9,10]. EBV needs to ensure that EBNA1-expressing cells are not detected and destroyed by the immune system and it has previously been shown that EBNA1 uses a mechanism based on minimizing EBNA1 synthesis to evade MHC class I pathway and $CD8^+$ T cell recognition. At the same time, EBNA1's low turnover rate ensures that a sufficient amount of EBNA1 is expressed to support the

virus [36]. The inhibition of synthesis and stability are both mediated by the GAr sequence [7]. However, although autophagy has been shown to contribute to the processing of EBNA1 for the MHC class II pathway [12], our data suggest that this mechanism is not involved in the production of EBNA1-derived substrates for the MHC class I pathway. This raises the possibility that EBNA1 has evolved a mechanism to specifically evade autophagy-mediated class I- but not class II-restricted antigen presentation. In line with the notion of an active EBNA1–mediated mechanism to evade class I-restricted antigen presentation, we observed that when the GAr is fused to OVA it prevents OVA from being presented via autophagy. This suggests that evasion of autophagy-mediated MHC class I-restricted antigen presentation is another mechanisms employed by viruses to remain undetected by the immune system.

Although the fusion of the PolyQ sequence to the OVA led to the formation of aggregates, it did not alter Atg5/12-dependent change in MHC class I-restricted antigen presentation, suggesting that aggregates alone is not the key to antigen presentation via autophagy. This is supported by the observation that OVA alone, nor EBNA1, results in any obvious aggregate formation, at least which could be detected by the methods used here. Nevertheless, it is interesting that the disordered gly-ala domain that is known to affect protein folding and unfolding, [24] prevents presentation to the class I pathway via synthesis and autophagy suppression. If this reflects a more general mechanism to evade the class I pathway, or if it is restricted to the GAr, remains to be seen. The reporter constructs we used carries the PolyQ and the GAr sequences in the N-termini of the OVA reporter constructs and even though the GAr is located inside the EBNA1 protein, it is possible that the location of

the GAr and the PolyQ can affect how substrates are presented to the class I pathway via autophagy.

By inserting *c-myc* 5' UTR upstream of GAr-carrying constructs we could override its translation inhibitory capacity and show that protein expression levels have little effect on GAr-mediated evasion of antigen presentation via autophagy. This points towards a more selective mechanism for how peptide substrates are presented to the class I pathway by autophagy and has interesting implications for understanding not only the cell biological aspects of how proteins are processed by autophagy, but also in terms of disease etiology. Animal studies have suggested that the inflammasome plays a role in Alzheimer disease, indicating that the immune response can play a role in the etiology of neurological disease associated with protein aggregates [37,38]. It is an interesting possibility that there could be a selective autophagy-dependent processing of cellular disease-associated substrates for the MHC I and II pathways. Further studies using more substrates and deeper analysis of autophagy pathways shall confirm, or not, this possibility. The implication of autophagy in the clearence of intracellular protein aggregates associated with poluglutamine disorders such as Hungtington disease (HD) is known [15] and Qin and colleagues showed that autophagy inhibition reduced cell viability and increased Huntingtin protein aggregation[34].

It is unlikely that the knock down of Atg5/12 affects the MHC class I pathway *per se* as the effect we observed are substrate-specific and secondly, that the addition of synthetic SL8 peptide to the Kb class I molecules did not show any difference during Atg5/12 knock down (**Supplementary Fig. 6A**) and neither in the membrane location of endogenous MHC-I Kb molecules in murine MCA-205 cells or HLA-ABC molecules in human H1299 cells (**Supplementary Fig. 6B**).

In line with our results, Liu and colleagues implicated OVA as being a substrate for autophagy and showed that mice immunized with OVA caused an allergy reaction and induced activation of autophagy accompanied by a relative increase of LC3 II compared to LC3 I in eosinophils cells from lung tissues [39]. Our study shows autophagy-dependent presentation of OVA for the direct class I pathway but other studies have associated autophagy with cross-presentation via uptake of substrates by dendritic cells. For example, polyQ fused to OVA was shown to be presented to the MHC class I pathway following injection into mice[30].

Taken together, this study shows a substrate-specific presention of peptides via autophagy that is selective for the MHC class I pathway. it has interesting implications for viral immune evasion and for inflammatory reactions associated with disease in which cellular proteins are processed by autophagy.

Acknowledgements

This work was partially supported by Inserm, European Regional Development Fund (ENOCH, CZ.02.1.01/0.0/0.0/16_019/0000868), MH CZ – DRO (MMCI, 00209805), Cancerforskningsfonden Norr, Cancerfonden (160598), Vetenskapsradet and by the International Centre for Cancer Vaccine Science within the International Research Agendas program of the Foundation for Polish Science co-financed by the European Union under the European Regional Development Fund.

References

[1] J. Neefjes, M.L.M. Jongsma, P. Paul, O. Bakke, Towards a systems understanding of MHC class I and MHC class II antigen presentation, Nat. Rev. Immunol. 11 (2011) 823–836. https://doi.org/10.1038/nri3084.

[2] J.W. Yewdell, D. Dersh, R. Fåhraeus, Peptide Channeling: The Key to MHC Class I Immunosurveillance?, Trends Cell Biol. 29 (2019) 929–939. https://doi.org/10.1016/j.tcb.2019.09.004.

[3] J. Wei, R.J. Kishton, M. Angel, C.S. Conn, N. Dalla-Venezia, V. Marcel, A. Vincent, F. Catez, S. Ferré, L. Ayadi, V. Marchand, D. Dersh, J.S. Gibbs, I.P. Ivanov, N. Fridlyand, Y. Couté, J.J. Diaz, S.B. Qian, L.M. Staudt, N.P. Restifo, J.W. Yewdell, Ribosomal Proteins Regulate MHC Class I Peptide Generation

for Immunosurveillance, Mol. Cell. 73 (2019) 1162-1173.e5. https://doi.org/10.1016/j.molcel.2018.12.020.

[4] S. Apcher, C. Daskalogianni, F. Lejeune, B. Manoury, G. Imhoos, L. Heslop, R. Fahraeus, Major source of antigenic peptides for the MHC class I pathway is produced during the pioneer round of mRNA translation, Proc. Natl. Acad. Sci. 108 (2011) 11572–11577. https://doi.org/10.1073/pnas.1104104108.

[5] S. Apcher, G. Millot, C. Daskalogianni, A. Scherl, B. Manoury, R. Fahraeus, Translation of pre-spliced RNAs in the nuclear compartment generates peptides for the MHC class I pathway, Proc. Natl. Acad. Sci. 110 (2013) 17951–17956. https://doi.org/10.1073/pnas.1309956110.

[6] E. Duvallet, M. Boulpicante, T. Yamazaki, C. Daskalogianni, R. Prado Martins, S. Baconnais, B. Manoury, R. Fahraeus, S. Apcher, Exosome-driven transfer of tumor-associated Pioneer Translation Products (TA-PTPs) for the MHC class I cross-presentation pathway, Oncoimmunology. 5 (2016) 1–15. https://doi.org/10.1080/2162402X.2016.1198865.

[7] Y. Yin, B. Manoury, R. Fåhraeus, Self-inhibition of synthesis and antigen presentation by Epstein-Barr virus-encoded EBNA1, Science (80-.). 301 (2003) 1371–1374. https://doi.org/10.1126/science.1088902.

[8] H.J. Kwun, S.R. da Silva, I.M. Shah, N. Blake, P.S. Moore, Y. Chang, Kaposi's Sarcoma-Associated Herpesvirus Latency-Associated Nuclear Antigen 1 Mimics Epstein-Barr Virus EBNA1 Immune Evasion through Central Repeat Domain Effects on Protein Processing, J. Virol. 81 (2007) 8225–8235. https://doi.org/10.1128/jvi.00411-07.

[9] J. Luka, T. Lindahl, G. Klein, Purification of the Epstein-Barr virus-determined nuclear antigen from Epstein-Barr virus-transformed human lymphoid cell lines., J. Virol. 27 (1978) 604–611. https://doi.org/10.1128/jvi.27.3.604-611.1978.

[10] K. Hennessy, E. Kieff, One of two Epstein-Barr virus nuclear antigens contains a glycine- alanine copolymer domain, Proc Natl Acad Sci U S A. 80 (1983) 5665–5669.

[11] S. Apcher, A. Komarova, C. Daskalogianni, Y. Yin, L. Malbert-Colas, R. Fåhraeus, mRNA Translation Regulation by the Gly-Ala Repeat of Epstein-Barr Virus Nuclear Antigen 1, J. Virol. 83 (2009) 1289–1298. https://doi.org/10.1128/jvi.01369-08.

[12] C. Paludan, D. Schmid, M. Landthaler, M. Vockerodt, D. Kube, T. Tuschl, C. Münz, Endogenous MHC class II processing of a viral nuclear antigen after autophagy, Science (80-.). 307 (2005) 593–596. https://doi.org/10.1126/science.1104904.

[13] C.C. Oliveira, T. Van Hall, Importance of TAP-independent processing pathways, Mol. Immunol. 55 (2013) 113–116. https://doi.org/10.1016/j.molimm.2012.10.005.

[14] S.K. Tey, R. Khanna, Autophagy mediates transporter associated with antigen processing- independent presentation of viral epitopes through MHC class I pathway, Blood. 120 (2012) 994–1004. https://doi.org/10.1182/blood-2012-01-

402404.

[15] Q. Zheng-Hong, Autophagy: biology and diseases, 2019.

[16] D.G. Mcewan, Host – pathogen interactions and subversion of autophagy, 0 (2017) 687–697.

[17] M. Mehrpour, A. Esclatine, I. Beau, P. Codogno, Overview of macroautophagy regulation in mammalian cells, Cell Res. 20 (2010) 748–762. https://doi.org/10.1038/cr.2010.82.

[18] V. Kirkin, V. V. Rogov, A Diversity of Selective Autophagy Receptors Determines the Specificity of the Autophagy Pathway, Mol. Cell. 76 (2019) 268–285. https://doi.org/10.1016/j.molcel.2019.09.005.

[19] D. Gatica, V. Lahiri, D.J. Klionsky, Cargo recognition and degradation by selective autophagy, Nat. Cell Biol. 20 (2018) 233–242. https://doi.org/10.1038/s41556-018-0037-z.

[20] I. Dikic, Z. Elazar, Mechanism and medical implications of mammalian autophagy, Nat. Rev. Mol. Cell Biol. 19 (2018) 349–364. https://doi.org/10.1038/s41580-018-0003-4.

[21] N. Mizushima, M. Komatsu, Autophagy: Renovation of cells and tissues, Cell. 147 (2011) 728–741. https://doi.org/10.1016/j.cell.2011.10.026.

[22] V.L. Crotzer, J.S. Blum, Autophagy and adaptive immunity, Immunology. 131 (2010) 9–17. https://doi.org/10.1111/j.1365-2567.2010.03321.x.

[23] S. Apcher, C. Daskalogianni, B. Manoury, R. Fåhraeus, Epstein barr virus-encoded EBNA1 interference with MHC class I antigen presentation reveals a close correlation between mRNA translation initiation and antigen presentation, PLoS Pathog. 6 (2010) 1–14. https://doi.org/10.1371/journal.ppat.1001151.

[24] C. Daskalogianni, S. Apcher, M.M. Candeias, N. Naski, F. Calvo, R. Fåhraeus, Gly-Ala repeats induce position- and substrate-specific regulation of 26 S proteasome-dependent partial processing, J. Biol. Chem. 283 (2008) 30090–30100. https://doi.org/10.1074/jbc.M803290200.

[25] E.L. Axe, S.A. Walker, M. Manifava, P. Chandra, H.L. Roderick, A. Habermann, G. Griffiths, N.T. Ktistakis, Autophagosome formation from membrane compartments enriched in phosphatidylinositol 3-phosphate and dynamically connected to the endoplasmic reticulum, J. Cell Biol. 182 (2008) 685–701. https://doi.org/10.1083/jcb.200803137.

[26] R.P. Martins, S. Findakly, C. Daskalogianni, M.P. Teulade-Fichou, M. Blondel, R. Fåhraeus, In cellulo protein-mRNA interaction assay to determine the action of G-quadruplex-binding molecules, Molecules. 23 (2018). https://doi.org/10.3390/molecules23123124.

[27] M. Noboru, T. Yoshimorim, B. Levine, Methods in Mammalian Autophagy Researvh, Cell. 140 (2010) 313–326. https://doi.org/10.1016/j.cell.2010.01.028.Methods.

[28] H.K. Lee, L.M. Mattei, B.E. Steinberg, P. Alberts, Y.H. Lee, A. Chervonsky, N. Mizushima, S. Grinstein, A. Iwasaki, In Vivo Requirement for Atg5 in Antigen

Presentation by Dendritic Cells, Immunity. 32 (2010) 227–239. https://doi.org/10.1016/j.immuni.2009.12.006.

[29] L. Tabe, P. Krieg, R. Strachan, D. Jackson, E. Wallis, A. Colman, Segregation of mutant ovalbumins and ovalbumin-globin fusion proteins in Xenopus oocytes. Identification of an ovalbumin signal sequence, J. Mol. Biol. 180 (1984) 645–666. https://doi.org/10.1016/0022-2836(84)90031-7.

[30] S. Tabachnick-Cherny, S. Pinto, D. Berko, C. Curato, Y. Wolf, Z. Porat, R. Karmona, B. Tirosh, S. Jung, A. Navon, Polyglutamine-Related Aggregates Can Serve as a Potent Antigen Source for Cross-Presentation by Dendritic Cells, J. Immunol. 205 (2020) 2583–2594. https://doi.org/10.4049/jimmunol.1901535.

[31] S.T. Suhr, M.C. Senut, J.P. Whitelegge, K.F. Faull, D.B. Cuizon, F.H. Gage, Identities of sequestered proteins in aggregates from cells with induced polyglutamine expression, J. Cell Biol. 153 (2001) 283–294. https://doi.org/10.1083/jcb.153.2.283.

[32] A. Ashkenazi, C.F. Bento, T. Ricketts, M. Vicinanza, F. Siddiqi, M. Pavel, F. Squitieri, M.C. Hardenberg, S. Imarisio, F.M. Menzies, D.C. Rubinsztein, Polyglutamine tracts regulate beclin 1-dependent autophagy, Nature. 545 (2017) 108–111. https://doi.org/10.1038/nature22078.

[33] A.R. La Spada, J.P. Taylor, Repeat expansion disease: Progress and puzzles in disease pathogenesis, Nat. Rev. Genet. 11 (2010) 247–258. https://doi.org/10.1038/nrg2748.

[34] Z.H. Qin, Y. Wang, K.B. Kegel, A. Kazantsev, B.L. Apostol, L.M. Thompson, J. Yoder, N. Aronin, M. DiFiglia, Autophagy regulates the processing of amino terminal huntingtin fragments, Hum. Mol. Genet. 12 (2003) 3231–3244. https://doi.org/10.1093/hmg/ddg346.

[35] C. Münz, Epstein Barr Virus Volume 2: One Herpes Virus: Many Diseases, Springer US, 2015. https://doi.org/10.3109/08820137709055812.

[36] J.B. Wilson, E. Manet, H. Gruffat, P. Busson, M. Blondel, R. Fahraeus, EBNA1: Oncogenic activity, immune evasion and biochemical functions provide targets for novel therapeutic strategies against epstein-barr virus-associated cancers, Cancers (Basel). 10 (2018) 1–29. https://doi.org/10.3390/cancers10040109.

[37] H. Du, M.Y. Wong, T. Zhang, M.N. Santos, C. Hsu, J. Zhang, H. Yu, W. Luo, F. Hu, A multifaceted role of progranulin in regulating amyloid-beta dynamics and responses, Life Sci. Alliance. 4 (2021) 1–22. https://doi.org/10.26508/lsa.202000874.

[38] J. Yang, L. Wise, K.I. Fukuchi, TLR4 Cross-Talk With NLRP3 Inflammasome and Complement Signaling Pathways in Alzheimer's Disease, Front. Immunol. 11 (2020) 1–16. https://doi.org/10.3389/fimmu.2020.00724.

[39] J.N. Liu, D.H. Suh, H.K.T. Trinh, Y.J. Chwae, H.S. Park, Y.S. Shin, The role of autophagy in allergic inflammation: A new target for severe asthma, Exp. Mol. Med. 48 (2016) e243-10. https://doi.org/10.1038/emm.2016.38.

Figures legends

Figure 1. *Autophagy Inhibition*. **A.** The *Atg5/12* mRNA levels were confirmed using RT-qPCR seventy-two hours following transfection of [20 pM] human siRNA against Atg5/12 or scramble siRNA **B.** Western Blots show the expression of Atg12, LC3 I and LC3 II. Values above the bands show the densitometry analysis normalized against β-actin and the fold change compared with the scramble siRNA. Autophagy suppression was estimated by the ratio between LC3 II and LC3 I **C.** H1299 cells were transfected with a plasmid encoding LC3-GFP 24 hours after treatment with siRNAs as in A and B. 48 hours later, cells were treated without serum during two hours and then fixed. One of 10 fields is shown from one of three similar experiments. LC3-GFP fluorescence was observed as green dots, indicating autophagosomes formation. Number of GFP dots was calculated (top right graph). LC3-GFP expression was determined by Western Blot (bottom panels). Values above the bands show the densitometry analysis of bands normalized with β-actin and the fold change comparing the complete medium with the serum starvation treatment. Significant values were calculated using Multiple paired T test grouped. ***P < 0.0002; **P < 0.0021; 0,1234 ns, not significant. White scale bars denote 10 µm.

Figure 2. *Autophagy affects antigen presentation of Ovalbumin and Ovalbumin fused to the poly glutamine peptide* **A.** Cartoon illustrating chicken ovalbumin (OVA) sequence with the location of the immune peptide SL8 and the glutamine repeat (PolyQ) **B.** Representative immunofluorescence image of OVA and PolyQ-OVA. White arrows heads indicate aggregation pattern. The graph shows the average number of aggregates observed **C.** Western Blot showing the effect of 72 hours Atg5/12 human siRNA transfection on OVA and PolyQ-OVA expression. The graphs below show the densitometry analysis, normalized against β-actin and expressed in fold change

compared with the scramble siRNA **D.** H1299 were transfected with human siRNA Atg5/12 [20 pM] or scrambled siRNA. 24 hours later they were transfected with murine MHC-I (kb) and indicated constructs. After 48 hours they were incubated with OT-1 $CD8^+$ T cells labeled with cell-trace violet for another 48 hours. OT-1 $CD8^+$ T cell proliferation was analyzed by flow cytometry. Higher rate of proliferation indicates more antigen presentation. Open peaks in the histogram represent the proliferating populations and grey peaks denote unstimulated population (Empty Vector transfected cells) (left graph). The graph shows the sum of percentage of cells from generation 1 to 5 compared with percentage of non-dividing cells (generation 0) from 6 independent experiments (right graph). Significant values were calculated using Multiple paired T test grouped. *P < 0.0332; **P < 0.0021; ***P < 0.0002; ****P < 0.0001; 0,1234 ns, not significant. White scale bars denote 10 μm.

Figure 3. *Fusion of the EBNA1-derived gly-ala repeat (GAr) sequence suppresses Atg5/12-dependent antigen presentation*. **A.** Cartoon illustrating different EBNA1 constructs with, or without, the GAr (EBNA1ΔGAr) and GAr fused to Ovalbumin. The location of the nuclear localization signal (NLS), the DNA binding/dimerization sequence in EBNA1 and the SL8 epitope are indicated. **B.** Representative immunofluorescence image of EBNA1, EBNA1ΔGAr and GAr-OVA. **C.** H1299 cells co-expressing murine MHC-I (Kb) and the indicated constructs were transfected with human siRNA Atg5/12 [20 pM] or scramble siRNA during 72 hours like in figure 2D. The graph shows the percentage of cells from generation 1 to 5 compared with percentage of non-divided cells (generation 0) from 3 independent experiments (right graph) **D.** Western Blots show one out of three representative experiments on the effect of autophagy inhibition on EBNA1, EBNA1ΔGAr and GAr-OVA protein expression levels. The graphs show densitometry analysis normalized against β-actin and

expressed in fold change compared with the scramble siRNA. Significant values were calculated using Multiple paired T test grouped. Not significant ns: 0,1234. White scale bars denote 10 µm.

Figure 4. *Protein levels do not change autophagy-dependent antigen presentation*. **A.** Cartoon illustrating the location of *c-myc* 5' UTR RNA sequence inserted in the 5'UTR of EBNA1, EBNA1ΔGAr and GAr-OVA **B.** The *c-myc* fused to the 5' UTR of EBNA1, EBNA1ΔGAr and GAr-OVA constructs overcomes GAr-mediated mRNA translation suppression. Western blots show the differences in protein expression levels **C.** Representative immunofluorescence of EBNA1, EBNA1ΔGAr and GAr-OVA constructs carrying the *c-myc*. **D.** Western Blot showing the effect of autophagy inhibition on protein levels of the indicated constructs. The graphs show densitometry analysis, normalized against β-actin for all targeted proteins and expressed in fold change compared with the scramble siRNA. **E.** H1299 cells co-expressing murine MHC-I (Kb) and the indicated constructs following human siRNA Atg5/12 [20 pM] or scramble siRNA treatment during 72 hours. The antigen presentation was estimated as described in figures 2 and 3. The graph shows the percentage of cells from generation 1 to 5 compared with percentage of non-divided cells (generation 0) from 3 independent experiments (right graph). Significant values were calculated using Multiple paired T test grouped. Not significant ns: 0,1234. White scale bars denote 10 µm.

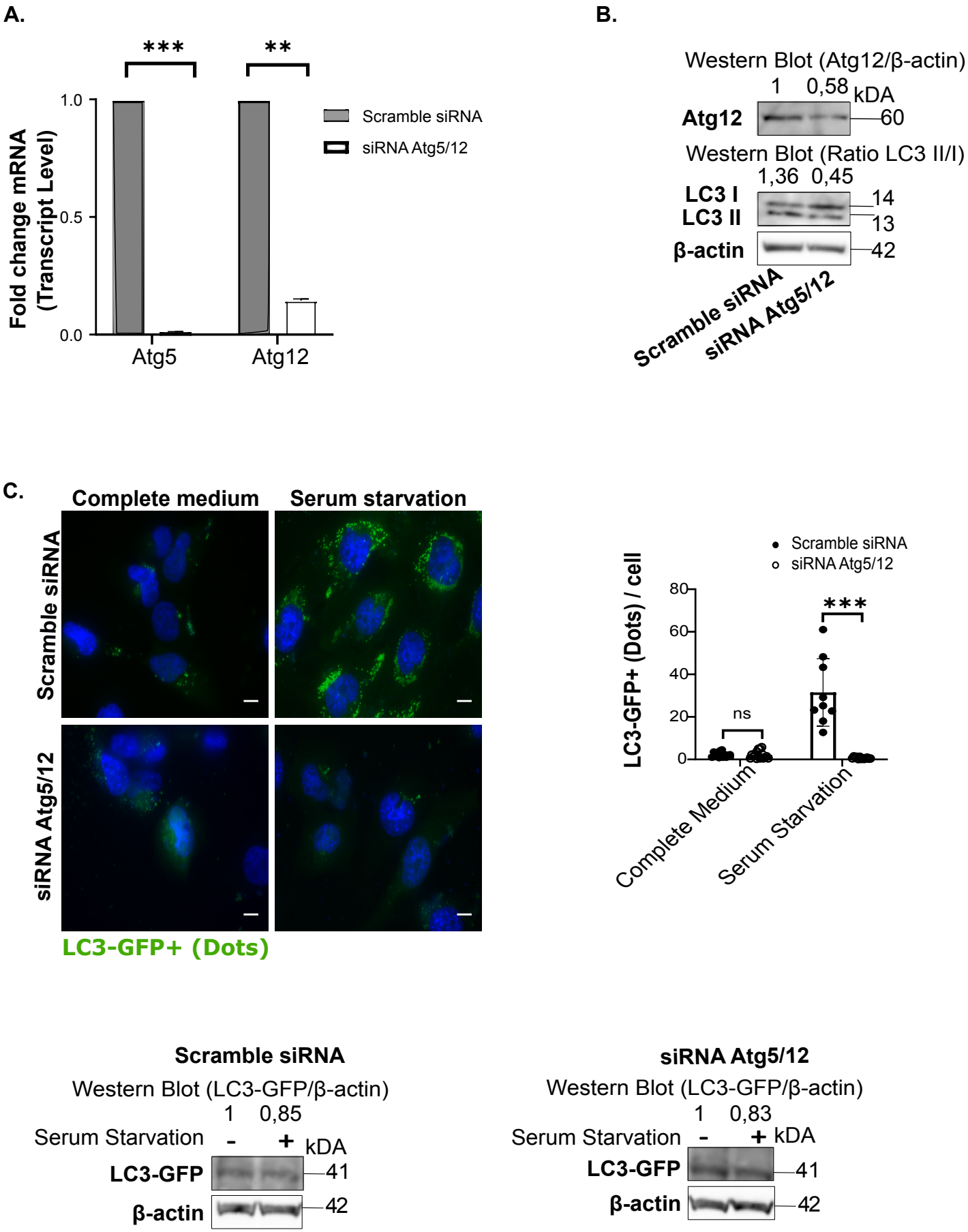

Figure 1 Color should be used in print

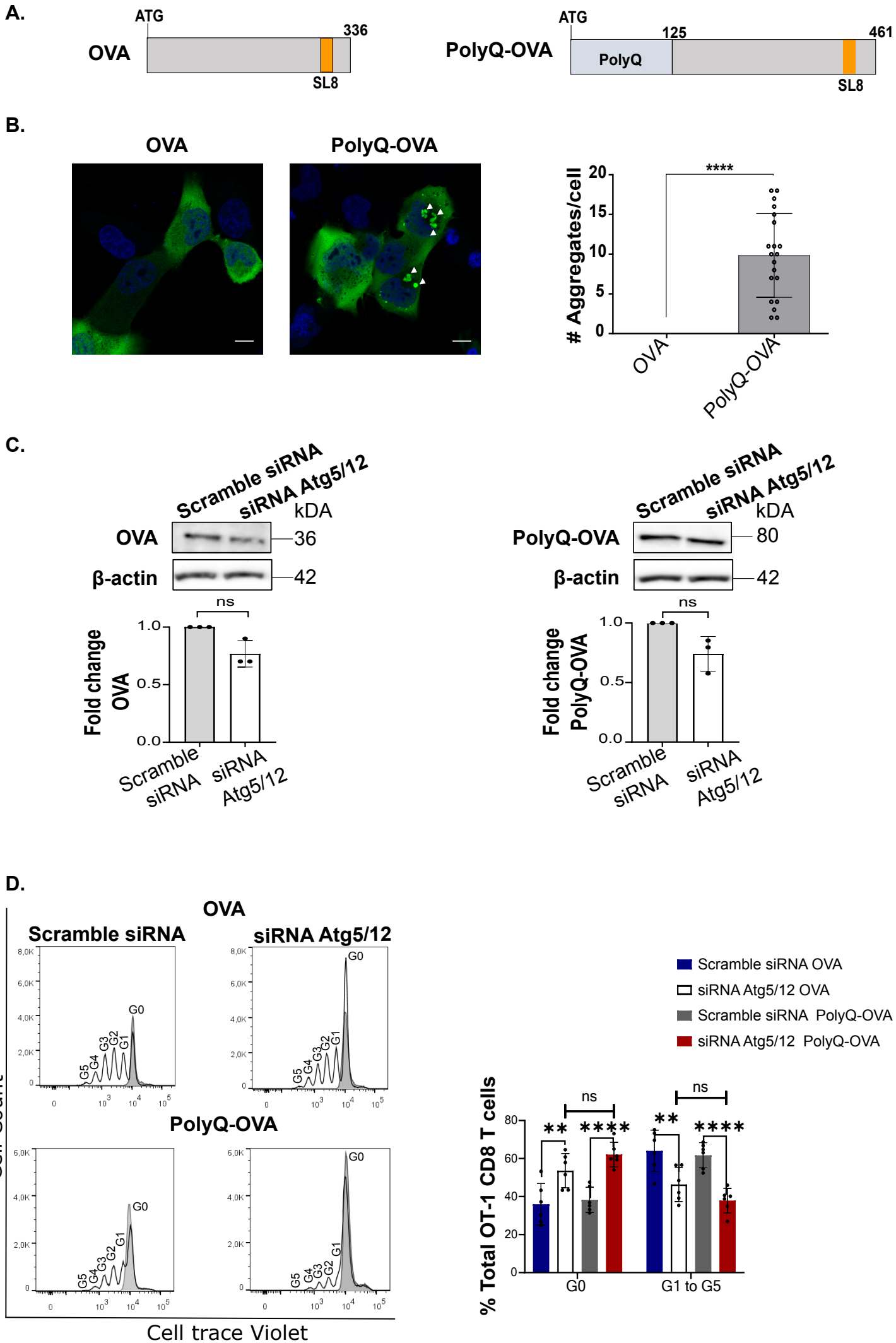

Figure 2 Color should be used in print

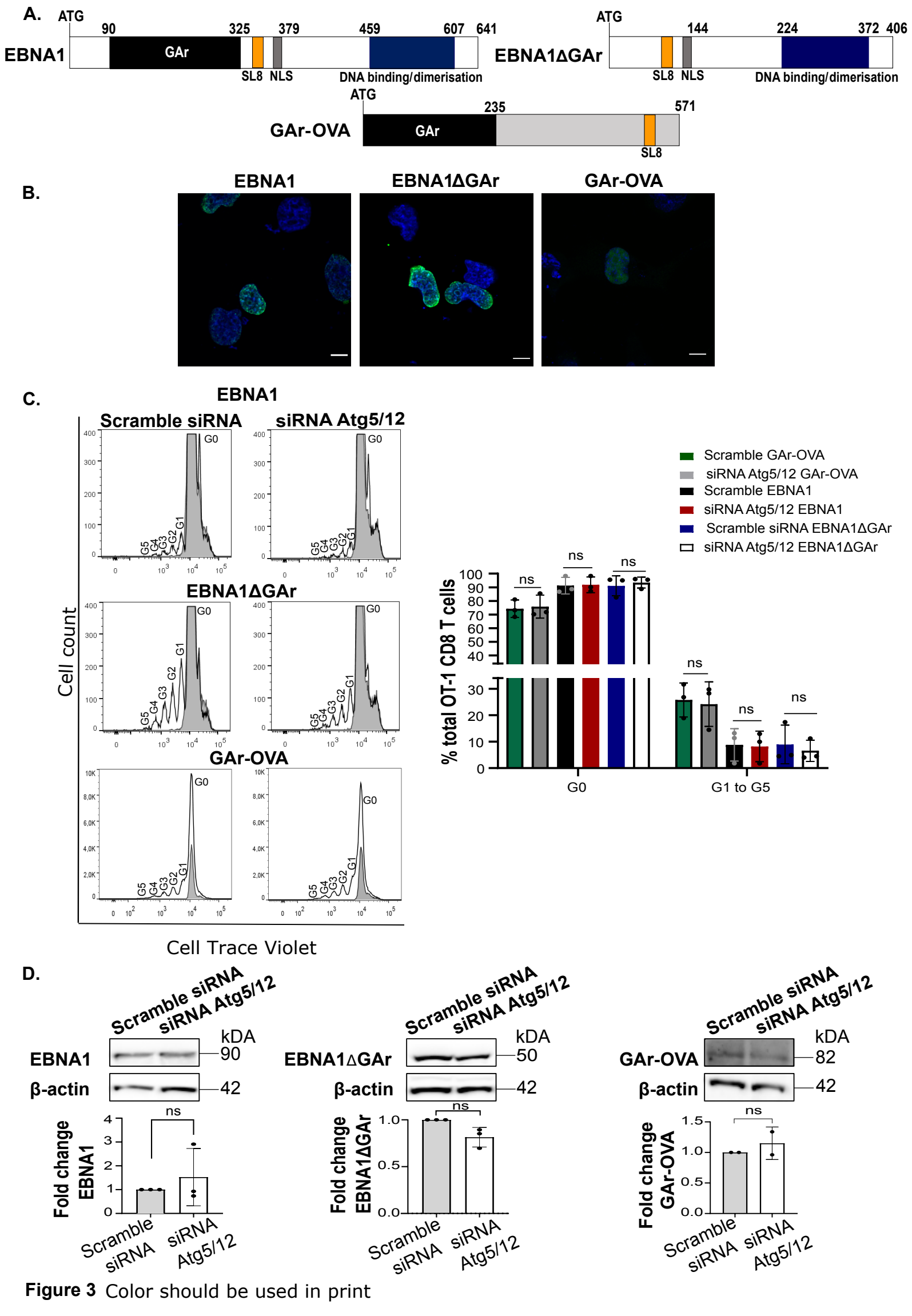

Figure 3 Color should be used in print

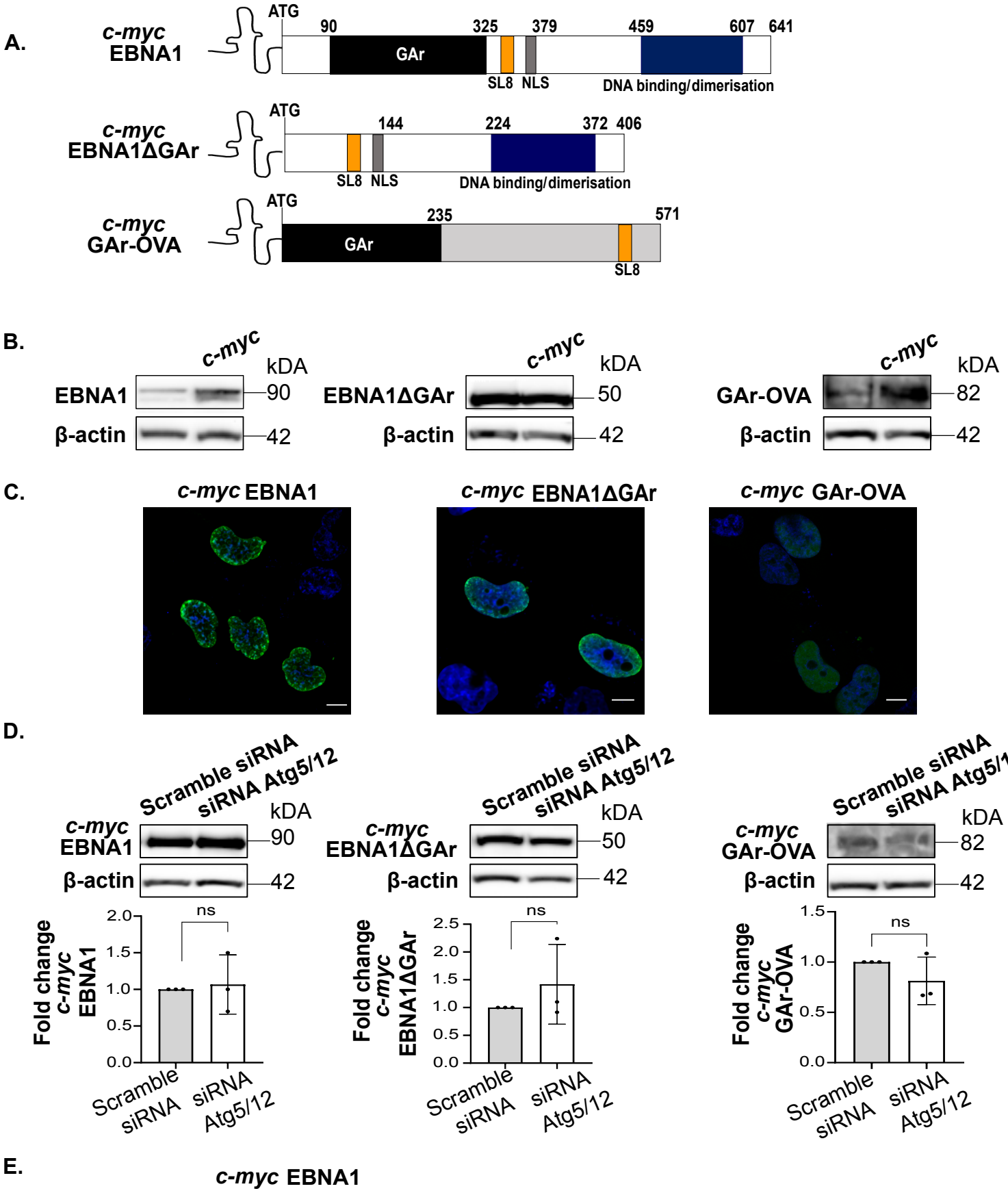

Figure 4 Color should be used in print